Crack detection in beam-like structures

Marta B. Rosales [a,b,*], Carlos P. Filipich [a,c], Fernando S. Buezas [b,d]

[a] *Department of Engineering, Universidad Nacional del Sur, Alem 1253, 8000 Bahía Blanca, Argentina*

[b] *CONICET, Argentina*

[c] *CIMTA - Centro de Investigaciones en Mecánica Teórica y Aplicada, FRBB, Universidad Tecnológica Nacional, 11 de Abril 465, 8000 Bahía Blanca, Argentina*

[d] *Department of Physics, Universidad Nacional del Sur, Alem 1253, 8000 Bahía Blanca, Argentina*

ABSTRACT

Sensibility analysis of experimentally measured frequencies as a criterion for crack detection has been extensively used in the last decades due to its simplicity. However the inverse problem of the crack parameters (location and depth) determination is not straightforward. An efficient numerical technique is necessary to obtain significant results. Two approaches are herein presented: The solution of the inverse problem with a power series technique (PST) and the use of artificial neural networks (ANNs). Cracks in a cantilever Bernoulli–Euler (BE) beam and a rotating beam are detected by means of an algorithm that solves the governing vibration problem of the beam with the PST. The ANNs technique does not need a previous model, but a training set of data is required. It is applied to the crack detection in the cantilever beam with a transverse crack. The first methodology is very simple and straightforward, though no optimization is included. It yields relative small errors in both the location and depth detection. When using one network for the detection of the two parameters, the ANNs behave adequately. However better results are found when one ANN is used for each parameter. Finally, a combination between the two techniques is suggested.

1. Introduction

Cracks in structural elements can indicate a fatigue problem, mechanical defects or others faults from the manufacturing process. In any case, they represent a threat to the reliable behavior of the part or structural element. Then their detection is a relevant issue. According to Rytter [1] the damage detection in a structure can be attained at four different levels: **Level 1**: detection of the existence of damage; **Level 2**: Level 1 plus damage location; **Level 3**: Level 2 plus damage quantification; **Level 4**: Level 3 plus prediction of the remaining service life (usually uncoupled from the other three levels). On the other hand, it is well known that a structural element shows changes in its behavior due to the presence of a crack. The estimation of the crack parameters (location and depth, Level 3) using the changes in the measured frequencies of a cracked member has been an extended criterion in the last decades. One of the reasons is that frequencies are, among other dynamic parameters, easily obtained from measurements. So their experimental determination for a given cracked element

is rather direct. However solving the inverse problem of crack parameters determination for a given set of frequencies in a damaged element can be a challenging task. Consequently, and in order to obtain meaningful results, both an acceptable model and an efficient numerical technique have to be adopted. Several researchers have tackled the problem with diverse techniques. Many works are available on crack detection in beams. Some representative papers are [2–7]. Shen and Taylor [7] report a procedure based on the minimization of the difference between measured data and a computational model to detect a crack in a Bernoulli–Euler beam. Liang et al. [5] develop theoretical relationships between eigenfrequency changes and magnitudes, and the locations of crack-induced damage for beam structures with either simply supported or cantilever boundary conditions. For uniform beams, a physical model of a massless rotational spring is used to represent the local flexibility introduced by the crack. Nandwana and Maiti [6] deal with inclined edge, or internal normal cracks using a rotational spring in slender beams. Bovsunovsky and Matveev [2] model a closing crack through a bilinear model of a cantilever Bernoulli–Euler beam. Kim et al. [3] present two damage detection methods, one based on frequencies and the other on mode shapes. Kim and Stubbs [4] use changes in natural frequencies of a structure as a practical method to detect cracks in beams. Fractional changes in modal energy are related to changes in natural frequencies due to damage.

* Corresponding author at: Department of Engineering, Universidad Nacional del Sur, Alem 1253, 8000 Bahía Blanca, Argentina. Tel.: +54 2914554423; fax: +54 2914595101.

E-mail address: mrosales@criba.edu.ar (M.B. Rosales).

In the present work, two approaches employing the frequency change criterion are explored. One is the solution of the inverse problem with a power series technique (PST) and the other is the use of artificial neural networks (ANNs). The power series algorithm is a systematization of this well-known technique which results in an efficient numerical method appropriate for this inverse problem. The authors have previously solved several ordinary nonlinear problems (both initial conditions and boundary value ones) using a similar approach [8]. Other boundary value problems were approached with power series [9]. The proposed methodology is straightforward and simple and, despite dealing with a linear model, the detection results are sufficiently accurate. Two structural elements are herein examined with PST: a Bernoulli–Euler (BE) beam and a spinning beam. The governing differential problem is stated and, in both cases, the crack is modeled by introducing springs of constant stiffness that vary for each crack size. First the analytic model of the BE beam with springs is stated and the differential problem is then solved by an algorithm based on power series which constitutes the direct problem. Since the aim is the detection of the damage up to level 3 (its existence, location and depth of the crack), an inverse problem should be tackled. The power series algorithm is then used to solve this inverse problem and, for this purpose, the natural frequencies measured in the damaged beam are input. The location and the value of the spring constant are the output, and a relationship from the Mechanics of Fracture theory [10] allows us to find the related crack depth. Both numerical and physical experiments are dealt with. The second application is related to the crack detection of a damaged spinning beam ("flexible rotor"). Similarly to the BE beam problem, the inverse problem solution leads to the determination of the crack parameters, and a detailed approach can be found in [11]. Finally the ANNs technique is applied to the case of the damaged cantilever beam. It differs from the previous approach since it does not involve governing equations but, on the other hand, needs a training set of data. A single hidden layer back-propagation neural network is trained with data found with 2D finite element models with more than four hundred scenarios. These data are also analyzed and some curves are depicted to show the variables' influence. Natural frequencies were measured from physical experiments and then input in the ANNs algorithm to detect the damage. First, one ANN to detect the two involved parameters was tested. Better results were found using two ANNs, detecting one parameter each [12]. A combination of the PST and ANN approaches is suggested.

2. Bernoulli–Euler beam-spring vibration problem

In the following sub-sections the natural vibration problem of a BE beam with an intermediate spring that represents the crack, will be stated. The direct approach and the power series solution will be presented.

2.1. BE beam with spring: Governing equations

In order to fix ideas, a cantilever cracked BE beam is considered (see Fig. 1). The crack influence is here simulated as a change in the flexibility at the crack location [5]. For this purpose, a spring of stiffness constant k^* is introduced. The beam has mass density ρ and Young's modulus E and, for the sake of generality, the beam is supposed to have two spans L_1 and L_2 of different cross sections F_1 and F_2 and second order moments of inertia J_1 and J_2, respectively. The governing equations of the natural transverse vibrations of the beam-spring system, after non-dimensionalization, are:

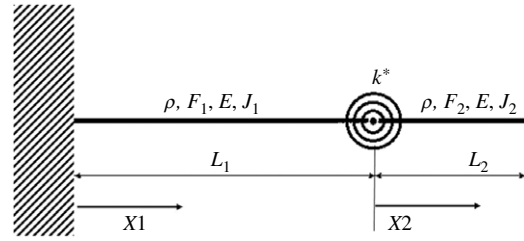$$v_1'''' - \Omega_1^2 v_1 = 0; \qquad v_2'''' - \Omega_2^2 v_2 = 0 \qquad (1)$$

Fig. 1. BE beam with an intermediate spring.

with the following boundary and continuity conditions

$$v_1(0) = 0; \qquad v_1'(0) = 0; \qquad v_2''(1) = 0; \qquad v_2'''(1) = 0$$

$$v_1(1) = v_2(0); \qquad \frac{EJ_1}{L_1} v_1''(1) + k \left[\frac{v_1'(1)}{L_1} - \frac{v_2'(0)}{L_2} \right] = 0. \qquad (2)$$

The following parameters have been introduced in order to obtain the non-dimensionalized governing equations: $x_1 = X_1/L_1, x_2 = X_2/L_2, 0 \leq X_1 \leq L_1, 0 \leq X_2 \leq L_2, 0 \leq x_1 \leq 1, 0 \leq x_2 \leq 1, \Omega_j^2 = \rho F_j \omega^2 L_j^4 / EJ_j$ $(j = 1, 2), k = k^* L_1 / EJ_1$ and where $v_1(x_1)$ and $v_2(x_2)$ are the *elastica* of each beam segment, ω is the circular frequency and Ω_1, Ω_2 are the two non-dimensionalized frequency parameters. The prime(s) in Eqs. (1) and (2) denote the derivative(s) with respect to x_1 or x_2 correspondingly.

2.2. Direct and inverse problem solutions via a power series algorithm for the BE beam

In the direct problem, the spring constant and its location are the input data, and the natural frequencies the output. Here the solution of the problem stated in Eqs. (1) and (2) is tackled *via* the PST. The power series is a very well-known technique and also straightforward. Its systematization yields an efficient method which is useful to afterwards solve the derived inverse problem. The unknowns are the functions $v_1(x_1)$ and $v_2(x_2)$ which are expanded as follows:

$$v_1(x_1) = \sum_i^N A_i x_1^i; \qquad v_2(x_2) = \sum_i^N B_i x_2^i;$$

$$N \to \infty \text{ (theoretically)} \qquad (3)$$

where A_i, B_i are unknowns $(i = 1, 2, \ldots, N)$. After introducing these expansions in Eqs. (1) and (2), the next relationships are obtained

$$B_0 = \sum A_i; \qquad \frac{k}{\alpha} B_1 = \sum \varphi_{2i} A_{i+2} + k \sum \varphi_{1i} A_{i+1};$$

$$2 \frac{\gamma}{\alpha^2} B_2 = \sum \varphi_{2i} A_{i+2}; \qquad 6 \frac{\gamma}{\alpha^3} B_3 = \sum \varphi_{3i} A_{i+3} \qquad (4)$$

$$A_{i+4} = \Omega_1^2 \frac{A_i}{\varphi_{4i}}; \qquad B_{i+4} = \Omega_2^2 \frac{B_i}{\varphi_{4i}}$$

where $\varphi_{ln} = (n + l)!/n!$ with l, n integer numbers. Also $\alpha = L_1/L_2, \beta = L_1/(L_1 + L_2), \gamma = EJ_2/(EJ_1)$. These are the necessary equations to construct the solution algorithm. The admissible input data are the spring constant k, the spring location β or the natural frequency parameters Ω's. Given two of them, the third can be obtained as an eigenvalue.

In order to solve the inverse problem, the first three natural frequencies of the damaged beam are obtained (either from a numerical or a physical experiment). After introducing each of these values in the power series algorithm (*input*), a curve β vs. k is obtained. The detected spring location and constant (*output*) are given by the intersection point of the three curves. The obtained value of β is proportional to L_1 (crack location) and the value of k is related to the crack depth by a relationship from Fracture Mechanics [10].
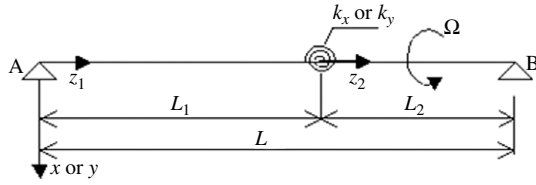
Fig. 2. Spinning beam with springs.

3. Spinning beam with spring vibration problem

This section includes the statement of the differential problem that governs the transverse vibrational problem of a spinning BE beam with and without intermediate springs.

3.1. Spinning beam governing equations

As stated in a previous work of the authors [13], the transverse, vibrational behavior of a beam rotating with constant spin about its longitudinal axis (z), assuming that its cross section (in the xy plane) possesses only one axis of symmetry, is governed by the following partial differential equations:

$$u'''' + a^2(\ddot{u} - \bar{\Omega}^2 u - 2\bar{\Omega}\dot{v}) = 0 \qquad (5)$$

$$v'''' + A^2(\ddot{v} - \bar{\Omega}^2 v + 2\bar{\Omega}\dot{u}) = 0 \qquad (6)$$

where, if z is coincident with the beam axis and the rotation is around it, $u(z, t)$ (in x direction) and $v(z, t)$ (in y direction) are the transverse displacements of the beam in plane xy of the cross section, $a^2 \equiv \rho F/EJ_x$, $A^2 \equiv \rho F/EJ_y$, ρ is the mass density of the beam, F is the cross-sectional area of the beam, J_x and J_y are the moments of inertia with respect to the x and y axes, respectively, E is the Young's modulus, $\bar{\Omega}$ is the constant angular velocity around the longitudinal axis z. Dots denote time differentiation and primes denote differentiation with respect to z. If normal modes are assumed Eqs. (5) and (6) can be written as

$$H'''' - a^2((\lambda^2 + \bar{\Omega}^2)H + 2\bar{\Omega}f) = 0 \qquad (7)$$

$$f'''' - A^2((\lambda^2 + \bar{\Omega}^2)f + 2\bar{\Omega}\lambda^2 H) = 0 \qquad (8)$$

where $H(z)$ and $f(z)$ are the mode shapes, unknowns of the problem. $\lambda's$ are the circular natural frequencies. These equations, together with the boundary conditions, are the basis of the stepped beam problem solved in the Appendix.

The vibration problem of a spinning beam with intermediate springs will be stated in the next section.

3.2. Spinning beam with intermediate springs

The spinning beam with intermediate springs is depicted in Fig. 2. The governing Eqs. (7) and (8) hold for each part of the beam: i.e. $H_1(z_1)$ and $f_1(z_1)$ for the first part and $H_2(z_2)$ and $f_2(z_2)$ for the second one, $0 \le z_j \le 1$, z_j are the non-dimensionalized variables ($j = 1, 2$). The boundary conditions for $H_1(z_1)$ and $H_2(z_2)$ are (assuming a simply supported beam)

$$H_1(0) = 0; \qquad H_2(1) = 0; \qquad H_1''(0) = 0; \qquad H_2''(1) = 0 \qquad (9)$$

and the continuity conditions are the following

$$H_1(1) = H_2(0); \qquad \frac{EJ_y}{L_1^3}H_1'''(1) - \frac{EJ_y}{L_2^3}H_2'''(0) = 0$$

$$\frac{EJ_y}{L_1^2}H_1''(1) + k_y\left[\frac{H_1'(1)}{L_1} - \frac{H_2'(0)}{L_2}\right] = 0 \qquad (10)$$

$$\frac{EJ_y}{L_2^2}H_2''(0) + k_y\left[\frac{H_1'(1)}{L_1} - \frac{H_2'(0)}{L_2}\right] = 0$$

where k_x and k_y are nondimensional spring constants, as defined in Section 2.1. Similar expressions are found for $f_1(z_1)$ and $f_2(z_2)$, respectively (not shown herein).

3.3. Solution of the spinning beam-springs vibration problem via PST

The basic unknowns in the direct problem are the mode shapes $H_1(z_1), H_2(z_2), f_1(z_1)$ and $f_2(z_2)$. They are expanded in power series, as follows:

$$H_j(z_j) = \sum_{i_0}^{\infty} A_{(j,i)}z_j^i \qquad f_j(z_j) = \sum_{i_0}^{\infty} B_{(j,i)}z_j^i \qquad (11)$$

where i_0 denotes $i = 0$, $i = 1, 2, \ldots, N$ $A(j, i)$ and $B(j, i)$ are unknowns and $j = 1, 2$. After the replacement of the expansions (11) in the differential system (7) and (10), the following recurrence system is obtained,

$$A_{(j,i+4)} = \frac{\Lambda_{y_j}[(1 + \eta^2)A_{(j,i)} - 2\eta B_{(j,i)}]}{\varphi_{4i}} \qquad (12)$$

$$B_{(j,i+4)} = \frac{\Lambda_{x_j}[(1 + \eta^2)B_{(j,i)} - 2\eta A_{(j,i)}]}{\varphi_{4i}} \qquad (13)$$

where:

$$\Lambda_{x_j} = \frac{\rho F L_j^4 \lambda^2}{EJ_x}; \qquad \Lambda_{y_j} = \frac{\rho F L_j^4 \lambda^2}{EJ_y}; \qquad \eta = \frac{\bar{\Omega}}{\lambda}$$

$$\varphi_{4i} = (i + 1)(i + 2)(i + 3)(i + 4) = \frac{(4 + i)!}{i!}.$$

The above-described algorithm is appropriate to solve the direct problem; i.e.: given a spinning beam with intermediate springs, the natural frequencies and mode shapes can be obtained. The same algorithm will be used to solve the inverse problem, as is described in the next subsection.

3.4. Inverse problem. Crack detection in a spinning beam

If one is able to measure the natural frequencies in a damaged spinning beam, then the previous algorithm gives a means to detect a crack, its location and its depth. At this stage of the study, and to validate the methodology, a numerical experiment is carried out in order to simulate it. A three-span beam is employed as a model of a cracked beam (see Appendix). The crack was assumed to be symmetric.

The spinning beam has a particular behavior, as reported by Bauer [14] and Filipich et al. [13], among other authors. For a given spin (angular velocity) the sequence of natural frequencies (ordered numerically), in general, alternate modes. Thus, if we choose an example (see Filipich et al. [13] and Rosales et al. [11]) ($J_x = J_y = J$, $\bar{\Omega}_{ND} = 70$, where $\bar{\Omega}_{ND} = \bar{\Omega}\sqrt{\frac{\rho F}{EJ}}$) the first frequency corresponds to the third mode (three semi-waves), the second frequency to the second (two semi-waves) and so on.

The detection methodology is similar to the one described for the BE beam. The "measured" frequencies are input in the power series algorithm and the respective curves β vs. k are obtained. The intersection point of the three curves represents the detected values. The obtained value of β is proportional to L_1 and the value of k is related to the crack depth. In this work, the spinning stepped beam model (see Appendix) was employed to tabulate different values of crack depths and the equivalent springs constants. The beam has three spans with flexural rigidity $(EJ_y)_i$, length L_i, transverse mode shapes H_i, spatial variable $0 \le z_i \le 1$, radius of cross-section d_i with $i = 1, 2, 3$. Since L_2 represents the crack width, it should have a very small value. An illustrative example will be shown below in the next Numerical examples section.
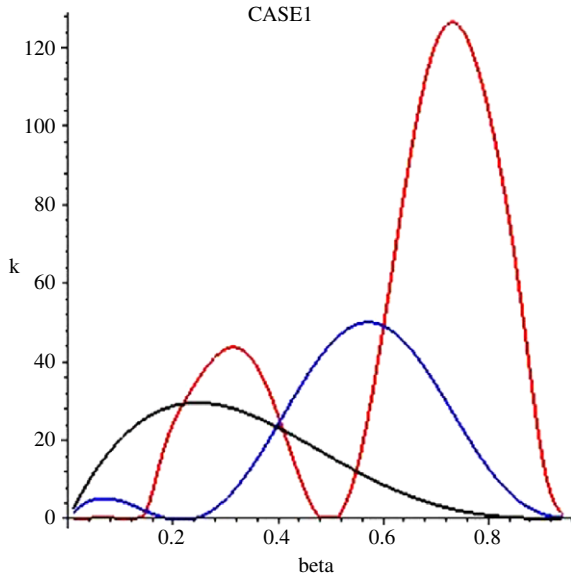
Fig. 3. Crack detection in a BE beam. Example 1: Numerical experiment. β–k curves.

4. Numerical examples using the power series technique (PST)

4.1. Results with PST: Cracked BE

In order to validate the proposed algorithm, two examples were solved, **Example 1:** a computational simulation of the cracked BE beam using a 2D finite element model and **Example 2:** a physical dynamic experiment of a damaged beam.

Example 1. *Detection using a computational simulation.* The crack was introduced as a notch and the standard finite element package ALGOR [15] was employed for the analysis. The data for the damaged beam with uniform cross-section is the following: length $L = 100$ cm, rectangular cross-section of height $h = 5$ cm and width $b = 1$ cm, Young's Modulus $E = 2.1 \times 10^{11}$ N/m^2 and Poisson's ratio $\nu = 0.3$. The frequency parameter is $\Omega = \omega L^2 \sqrt{\rho A/EJ}$. A *zero setting* correction is applied (see, for instance, Nandwana y Maiti [6]) to account for the discrepancies between the analytical BE beam and the computational 2D model. Such correction is done on each value of frequency. A cantilever beam is analyzed with three different values of the crack depth a, CASE 1 with $a = 1$ cm, CASE 2 with $a = 2$ cm, CASE 3 with $a = 3$ cm and in all the cases the 2D FEM was built for a cantilever beam with a notch 0.2 cm wide, located at $\beta = L_1/L = 0.4$. The first three natural frequencies are input in the power series algorithm, after the zero setting. Three curves k vs. β for each natural frequency are obtained. Fig. 3 shows the three curves obtained for CASE 1. It should be noted that curves for CASES 2 and 3 (not shown herein) are similar, though with different vertical scales. The intersection point gives the detected values of the parameters β and k and the value of the crack depth a can be estimated from the next relationship (Ostachowics y Krawczuk [10]) in which $r = a/h$ is the crack depth/section height ratio.

$$k = Ebh^2/[72\pi f(r)] \tag{14}$$
$$f(r) = 0.6384r^2 - 1.035r^3 + 3.7201r^4 - 5.1773r^5 + 7.553r^6 - 7.3324r^7 + 2.4909r^8.$$

Results and estimates ($\hat{L}_1$ and $\hat{a}$) for CASES 1, 2 and 3 are depicted in Table 1. The errors were calculated in such a way so that they are comparable, i.e.

$$\text{error}_{\hat{L}_1} = \frac{(\hat{L}_1 - L_1)}{L}; \qquad \text{error}_{\hat{a}} = \frac{(\hat{a} - a)}{h}. \tag{15}$$

Table 1
Bernoulli–Euler cantilever beam. Example 1. Crack parameter estimates $\hat{L}_1$ and $\hat{a}$ found using a numerical experiment. The percent errors calculated with Eq. (15) are shown between parentheses. $L = 1$ m, $L_1 = 0.4$ m, $b = 0.01$ m, $h = 0.05$ m.

CASE	Crack depth (m)	Ω_1	Ω_2	Ω_3	k	Estimated values	
						$\hat{L}_1$ (m)	$\hat{a}$ (m)
1	0.01	3.4905	21.7876	61.2885	23.63	0.4 (0%)	0.00906 (−1.88%)
2	0.02	3.3980	20.9411	59.9480	4.87	0.402 (0.2%)	0.01901 (−1.98%)
3	0.03	3.1526	19.1435	57.2844	1.41	0.4 (0%)	0.03111 (2.22%)

Table 2
BE beam physical experiment. Data for the different scenarios.

CASE	Crack width (m)	Crack location from free end (m)	Crack depth (m)
1	0.0013	0.2	0.0100
2	0.0015	0.3	0.0148
3	0.0014	0.2	0.0120

Table 3
Frequencies in Hz ($f_i = \omega_i/2\pi$) found with physical experiment and numerical simulation on cracked cantilever beam. $L = 0.40$ m.

Case	f_1	f_2	f_3	f_4
Non-damaged Exp	110	645	1845	3437
Non-damaged 2D FEM	113	689	1866	3515
1 Exp	105	565	1830	3225
1 2D FEM	110	609	1855	3390
2 Exp	85.5	610	1696	3325
2 2D FEM	80	664	1498	3461
3 Exp	109	580	1825	3275
3 2D FEM	107	566	1848	3388

Example 2. *Detection using a physical experiment.* Dynamic tests were performed on various specimens. In all the cases, the steel beam section was $b = 0.0223$ m and $h = 0.0223$ m. The beams were built with $L = 0.40$, 0.50, and 0.60 m. Table 2 depicts the experiment scenarios. To obtain the data, the equations of elasticity governing the beam plane stress problem were solved *via* a finite element method for different depths and locations of the crack using 2D finite elements with a quadratic finite element basis. Also Table 3 shows the experimentally measured natural frequencies for the beam of length $L = 0.40$ m. Measured frequencies are reported for Cases 1, 2 and 3. Also the non-damaged case is included as a reference. Additionally, the values of frequencies found with the numerical experiment using a 2D finite element model are depicted in the same table. Fig. 4 shows the variation of the natural frequencies for different values of the crack parameters (depth and location).

Finally, the frequency values measured in the experiments were input in the inverse PST algorithm. The resulting curves (similar to the ones reported in Fig. 3) are depicted in Fig. 5 for two of the analyzed cases. As before, the points at which the three curves intersect give the values of the location and the spring stiffness. After using Eq. (14) the crack parameters are found. The resulting estimates ($\hat{L}_1$ and $\hat{a}$) are listed in Table 4. The errors were calculated with expressions (15).

4.2. Results with PST: Cracked spinning beams

In order to test the usefulness of the technique, a crack detection example is now performed for a spinning beam. The simply-supported spinning beam has a circular cross-section of 0.05 m of radius ($J_x = J_y = J$) and length 1.00 m. The mass density is $\rho = 7850$ kg/m^3 and the Young's modulus is $E = 2.1 \times 10^{11}$ N/m^2. Two cases with different angular velocities are reported: $\bar{\Omega} = 3879.15$ rad/s and $\bar{\Omega} = 9051.34$ rad/s (which correspond to non-dimensional velocities $\bar{\Omega}_{ND} = 30$ and $\bar{\Omega}_{ND} = 70$ respectively).
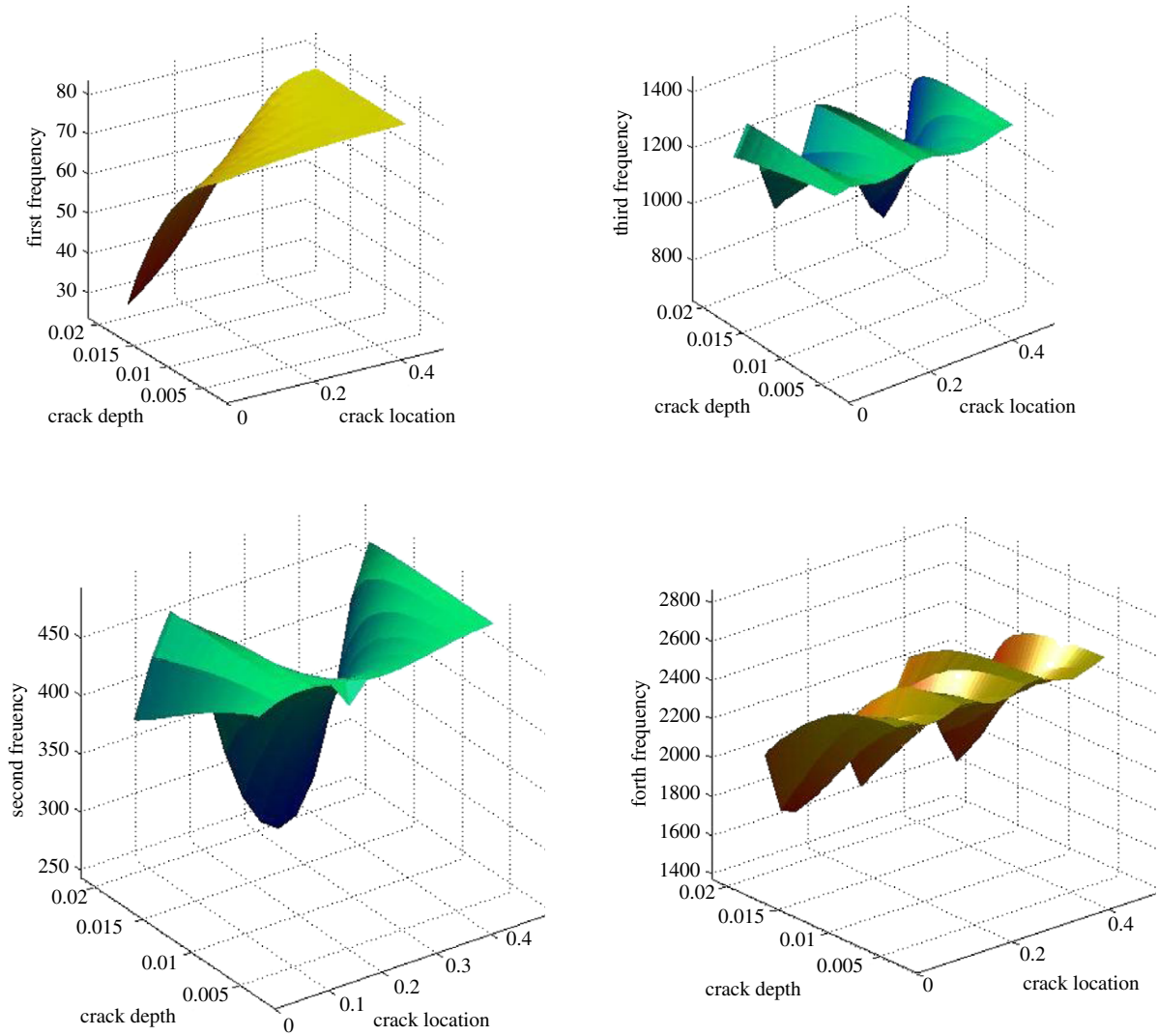
Fig. 4. Cracked BE beam. Variation of natural frequencies with crack depth and location. 2D finite element simulation.
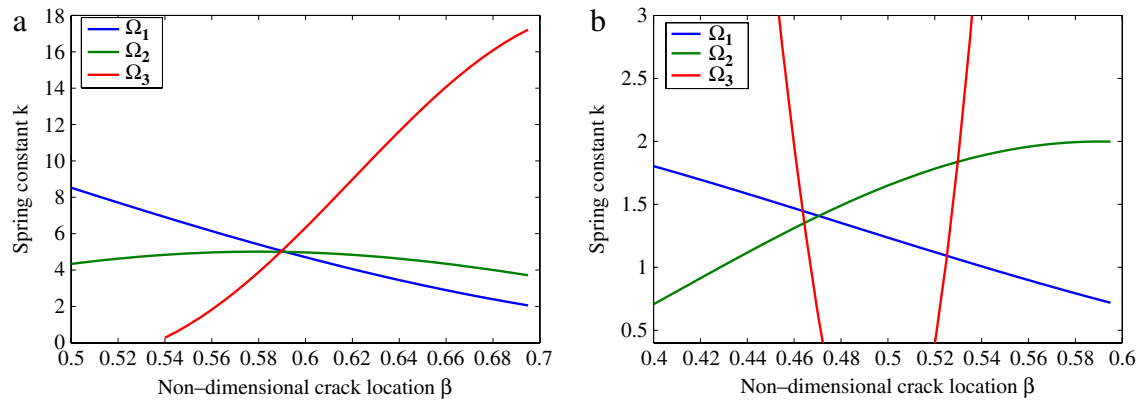

Fig. 5. Crack detection in a BE beam. Example 2: Physical experiment. β–k curves. (a) Case 1, $L = 0.50$ m, (b) Case 2, $L = 0.60$ m.

The cracked zone is modeled by a very short span $L_2 = 5 \times 10^{-4}$ m (see Appendix, Fig. A.1) wide and a circular cross-section of radius 0.03 m (i.e. a crack with depth $\bar{a} = 0.02$ m), located at 0.3 m from the left support (i.e. $z_1 = 0.3$ m in Fig. 2). The frequency values obtained for the damaged spinning beam of the present example (using the algorithm of the Appendix) are depicted in Tables 5 and 6, found with $\bar{\Omega}_{ND} = 30$ and $\bar{\Omega}_{ND} = 70$ respectively.

For each case, the first three values of frequencies are input in the beam-springs algorithm. As is observed in Tables 5 and 6, there are two different frequencies (among the first four ones) which correspond to the one semi-wave mode (see Section 3.4). It was found that both values lead to the same estimates of the crack parameters. Then, the three selected frequencies are corresponding to one, two and three semi-waves, respectively,

Table 4

Bernoulli–Euler cantilever beam. Example 2. Crack parameter estimates $\hat{L}_1$ and $\hat{a}$ found using a physical experiment. The percent errors calculated with Eq. (15) are shown between parentheses. $b = 0.0223$ m, $h = 0.0223$ m.

CASE (Table 2)	L (m)	Ω_1	Ω_2	Ω_3	k	Estimated values	
						$\hat{L}_1$ (m)	$\hat{a}$ (m)
1	0.4	3.3561	19.3016	61.1947	2.729	0.186 (3.5%)	0.0131 (13%)
1	0.5	3.4692	19.9138	59.1449	5.0169	0.295 (−1.0%)	0.0103 (1.3%)
3	0.5	3.4692	20.2759	60.0727	6.0128	0.285 (−3.0%)	0.0096 (−10%)
2	0.6	3.1058	20.4972	56.4295	1.4024	0.279 (−3.5%)	0.017 (9.8%)

which, in this particular problem of the spinning beam, are not in sequential order.

After the frequencies are input in the inverse algorithm, the intersection of the three curves L_1 (crack location) vs. k (spring stiffness) analog to the BE beam previously described, yields the solution of the crack detection problem. Due to the symmetry of the problem, two locations are found. In this case $L_1 = 0.3$ m and $L_1 = 0.7$ m (both at 0.3 m from the ends). The crack estimates $\hat{L}_1$ and $\hat{a}$ are shown in Table 7. In order to obtain the crack magnitude, a relationship between the springs constants and the crack depth should be used. Here, an energy approach using the stepped model of the Appendix was employed to tabulate different values of crack depths and the equivalent springs constants. By equating the bending energy with the external work, both within the intermediate span (the damaged zone) (Eq. (A.3)), one is able to find such a relationship. The estimates are, as expected, independent of the rotational velocity, and the error in the location estimate is negligible and acceptably low in the crack depth.

Table 7

Spinning beam. Crack parameters estimates using a numerical simulation. The percent errors calculated with Eq. (15) are shown between parentheses. $L = 1$ m, $h = 0.05$ m (radius).

$\bar{\Omega}_{ND}$	k	Estimated values	
		$\hat{L}_1$ (m)	$\hat{a}$ (m)
30	3.3985×10^8	0.3001 (0.01%)	0.0181 (−3.8%)
70	3.3985×10^8	0.3001 (0.01%)	0.0181 (−3.8%)

5. Artificial neural networks approach

The Artificial Neural Network (ANN) technique is a different approach [16]. It is inspired in the brain information processing through a very interconnected parallel structure. It does not involve governing equations but it needs a training set of data. The knowledge of the ANN is then acquired through a learning process in which both input and output (desired) data is supplied to the network. The so-called Multi-layer Perceptron architecture consists of a first layer with the input vector, a final layer with the output vector and intermediate layers (known as hidden layers) that link to the other layers through weighted connections. A simple representation of an ANN with a single hidden layer is depicted in Fig. 6. In this work, a single hidden layer and the backpropagation training algorithm are used. In this work, the ANN *learns* from the data consisting of more than four hundred scenarios from a computational experiment. Fig. 4 shows the results of the frequency values for all the studied cases, as described in previous Section 4.1.

As is usual, a portion of the data is chosen randomly to train the ANN (training set to fit the weights), and the other portion (20%) to validate the data. Several variables were modified such as

Table 5

First four natural frequencies of a cracked spinning beam. $\bar{\Omega}_{ND} = 30$.
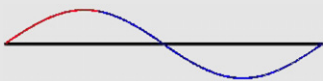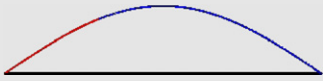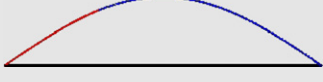
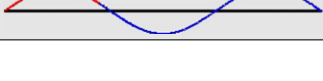| i	λ_i	Mode shape	Used
1	1211.71722951021		Yes
2	2605.48654642698		Yes
3	5152.80468312496		No
4	7603.25283041748		Yes

Table 6

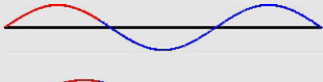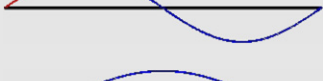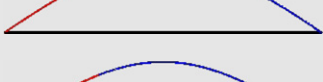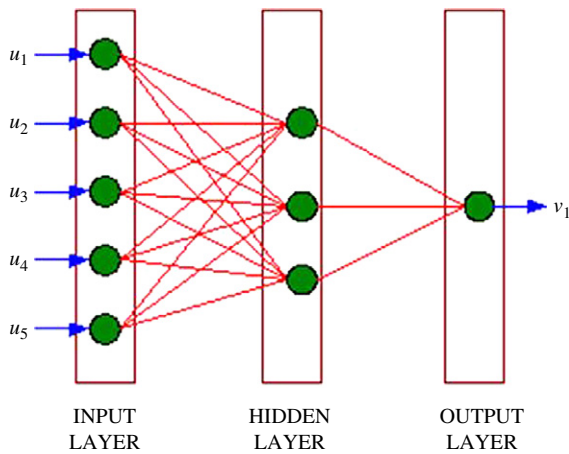First four natural frequencies of a cracked spinning beam. $\bar{\Omega}_{ND} = 70$.

i	λ	Mode shape	Used
1	2431.05867738177		Yes
2	3960.47692352495		Yes
3	7777.68069946014		Yes
4	10324.9988361644		No

Fig. 6. ANN scheme with input, hidden and output layer.

the number of neurons in the hidden layer, the learning rate, the number of samples for the validation. Fig. 7 shows an example of one of the output graphics obtained with the algorithm of training and validation after running 50 000 epochs (epoch is a step in the training process), with the first three natural frequencies as input and with three neurons in the hidden layer. It can be seen that the training and evaluation error are similar with no over-fitting. It was also observed that the input of the four frequencies, instead of three, in the training improved the performance. Also, two strategies were tested. First an ANN trained with the frequencies and both crack depth and location data. However, the handling of two output variables forces the ANN to accomplish a higher average error level. To overcome this situation, the authors propose

the finding of the crack location with the first technique PST and the crack depth with the ANNs.

Finally, results found with the physical experiments on a cracked cantilever beam detailed in Section 4.1 were introduced in the trained ANN algorithm. One of the cases is reported in Table 8. The length of the beam is $L = 0.50$ m, the crack is located at 0.30 m from the free end and it is 0.0148 m deep (Case 2, Table 2). The first four frequencies found by the physical experiment and input in the ANN algorithm to detect the crack are 67.5, 358, 1187 and 2300 Hz, respectively. First, a single ANN algorithm was used to handle the two parameters (location and depth), and then two algorithms, one for each parameter. The detected results improve in the second case.

Table 8
BE cantilever beam. ANN trained with computational data. Crack detection using experimentally measured natural frequencies. The percent errors calculated with Eq. (15) are shown between parentheses. $L = 0.5$ m, $L_1 = 0.2$ m, $a = 0.0148$ m.

Crack parameters (cm)	Case 3. Experimental data		
	One ANN two output $NN = 30$	Two ANN one output each $NN = 30$	Two ANN one output each $NN = 50$
Crack location $\hat{L}_1$	24.2 (−8.4%)	21.5 (−3%)	21.9 (−3.8%)
Crack depth $\hat{a}$	1.330 (−6.7%)	1.584 (4.6%)	1.457 (−1%)

6. Summary and conclusion

The detection of cracks for beam-type elements was addressed using the analysis of changes in the frequencies as a detection criterion. Two approaches were tackled, a power series technique (PST) and artificial neural networks (ANN). The use of PST provided
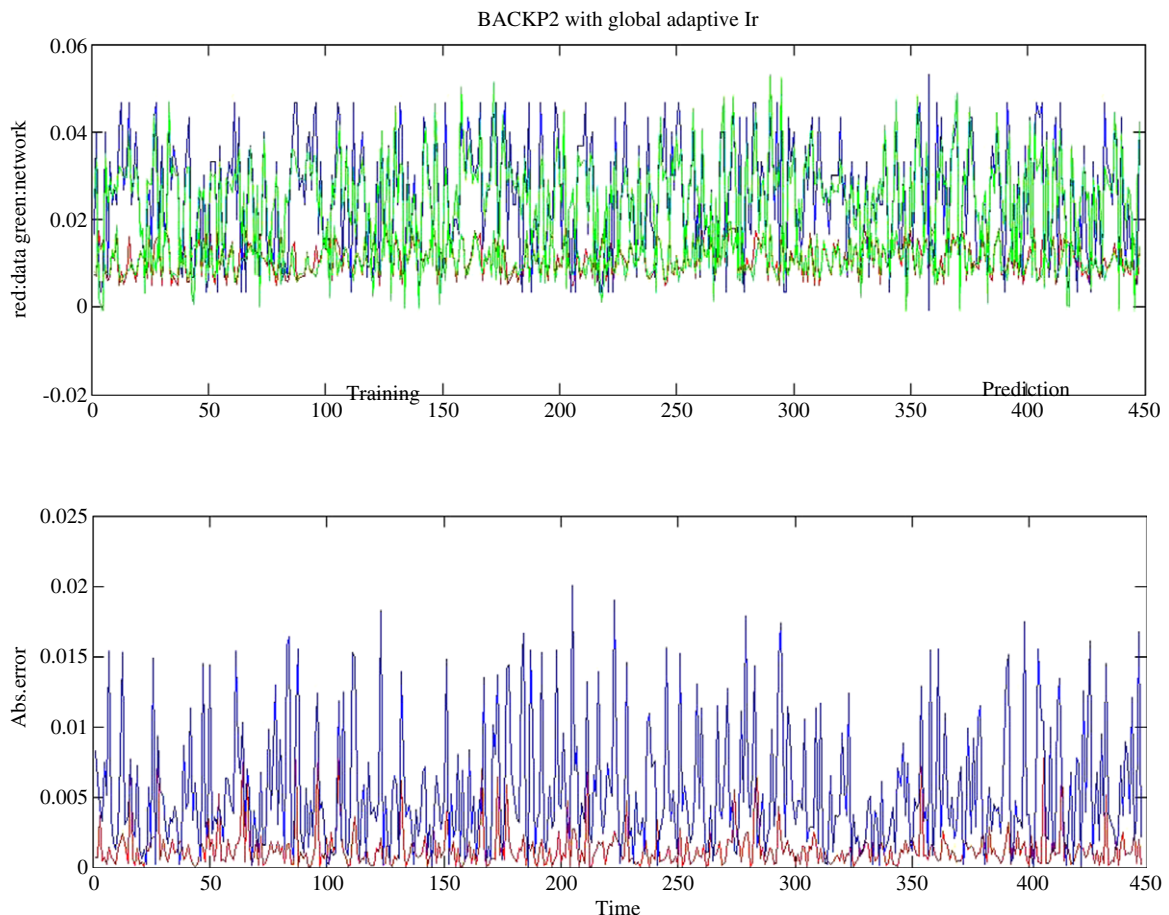

Fig. 7. ANN example of training and validations output. 50 000 epochs. Three neurons in the hidden layer.

a straightforward and efficient numerical technique to solve the inverse problem. The crack is modeled by introducing springs to represent the stiffness reduction. Two crack detecting problems were studied with PST: a Bernoulli–Euler cantilever beam and a spinning beam. The algorithm was tested with 2D computational experiments and physical experiments. The results are excellent in the location value and with acceptable errors in the depth for the first type of experiments. The error remains in an acceptable level when experimental data is employed. It was observed that the width of the crack (in the axis direction) affects the accuracy of the depth resulting value. This approach is proposed as a very simple technique to find a first approximation (recall that the algorithm solves a very simple beam model and without any optimization process) with almost no computational cost.

The ANN algorithm was implemented and trained with the numerical experiment data with a 2D finite element model of a cracked cantilever beam. Then, frequencies measured in a physical experiment were introduced in the trained ANN. Several examples were carried out and the results are satisfactory in general. However, a single ANN algorithm to handle the detection of the two parameters is not as efficient as two algorithms with one parameter each.

It can be concluded that the first proposed algorithm (Power Series Technique, PST) is very straightforward and detects the crack with very small errors and very low cost. However the simplicity of the model limits its use as an initial tool to make an economical detection at a first stage. Furthermore, the resulting estimates can be used as the seed to a more sophisticated methodology. The second algorithm (Artificial Neural Networks, ANN) yields on the average rather larger errors. However, the second approach might handle more complex models such as nonlinearities due to closing cracks or large deformations, subject to study by the authors [17].

Acknowledgments

Appendix

The vibrational problem of a stepped spinning beam of three spans (Fig. A.1) is governed by Eqs. (5) and (6), valid for each span. Once normal modes are assumed, Eqs. (7) and (8) must be solved for each span, where $H_1(z_1), f_1(z_1), H_2(z_2), f_2(z_2), H_3(z_3), f_3(z_3)$ are the mode shapes; $0 \leq z_j \leq 1$; $j = 1, 2, 3$.

The boundary conditions are:

$$H_1(0) = 0; \qquad H_3(1) = 0 H_1''(0) = 0; \qquad H_3''(1) = 0 \qquad \text{(A.1)}$$

and the continuity conditions are:

$$H_1(1) = H_2(0); \qquad H_2(1) = H_3(0)$$

$$\frac{H_1'(1)}{L_1} = \frac{H_2'(0)}{L_2}; \qquad \frac{H_2'(1)}{L_2} = \frac{H_3'(0)}{L_3}$$

$$\frac{EJ_y^1}{L_1^2} H_1''(1) = \frac{EJ_y^2}{L_2^2} H_2''(0); \qquad \frac{EJ_y^2}{L_2^2} H_2''(1) = \frac{EJ_y^3}{L_3^2} H_3''(0)$$

$$\frac{EJ_y^1}{L_1^3} H_1'''(1) = \frac{EJ_y^2}{L_2^3} H_2'''(0); \qquad \frac{EJ_y^2}{L_2^3} H_2'''(1) = \frac{EJ_y^3}{L_3^3} H_3'''(0).$$

Governing Eqs. (7) and (8) are written in terms of the unknowns (mode shapes H_j and f_j with $j = 1, 2, 3$). Similar boundary and continuity conditions exist for functions f_j. The system is then solved after proposing the following expansions in power series:
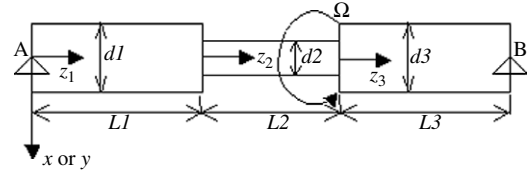

Fig. A.1. Stepped spinning beam.

$$H_j(z_j) = \sum_{i_0}^{\infty} A_{(j,i)} z_j^i; \qquad f_j(z_j) = \sum_{i_0}^{\infty} B_{(j,i)} z_j^i \quad j = 1, 2, 3. \qquad \text{(A.2)}$$

The natural frequencies and the corresponding mode shapes are then obtained for the desired geometry. In the present crack detection problem, the intermediate span represents the cracked section and consequently L_2 is assumed to be small. From this model, the equivalent spring constant of the second span (cracked section) can be found as follows:

$$\frac{(EJ_y')_2}{L_2^3} \int_0^1 [H_2'']^2 dz_2 = k_{eq} \frac{[H_2'(1) - H_2'(0)]^2}{L_2^2}. \qquad \text{(A.3)}$$

Then, for each value of crack depth a, i.e. $d_2 = d_1 - a$, it is possible to find the equivalent spring constant k_{eq}. Inversely, given a constant k, one is able to find the value of $J (=J_x = J_y)$ and from it, the corresponding radius of the intermediate span. The value of a is then derived directly. This appears as an alternative way to find a *k/crack depth* relationship necessary to detect the extension of the damage.

References

[1] Rytter A. Vibration based inspection of Civil Engineering structures. Ph.D. thesis. Denmark: Aalborg University; 1993.
[2] Bovsunovsky AP, Matveev VV. Analytical approach to the determination of dynamic characteristics of a beam with a closing crack. J Sound Vibr 2000; 235:415–34.
[3] Kim J-T, Ryu YS, Cho HM, Stubbs N. Damage identification in beam-type structures: Frequency-based method vs. mode-shape-based method. Eng Struct 2003;25:57–67.
[4] Kim J-T, Stubbs N. Crack detection in beam-type structures using frequency data. J Sound Vibr 2003;259:145–60.
[5] Liang RY, Hu J, Choi F. Theoretical study of crack-induced eigenfrequency changes on beam structures. J Eng Mech (ASCE) 1992;118:384–96.
[6] Nandwana BP, Maiti SK. Modeling of vibration of beam in presence of inclined edge or internal crack for its possible detection based on frequency measurements. Eng Fract Mech 1997;58:193–205.
[7] Shen M-HH, Taylor JE. An identification problem for vibrating cracked beams. J Sound Vibr 1991;150:457–84.
[8] Filipich CP, Rosales MB, Buezas FS. Some nonlinear mechanical problems solved with analytical solutions. Int J Latin Amer Appl Res 2004;34(2):105–23.
[9] Filipich CP, Bambill EA, Rosales MB. Pandeo de porticos planos. uso sistemático de series de potencias. In: ENIEF 2003. Rosales MB, Cortinez VH, Bambill DV, editors. Mecanica Computacional, vol. XXII. 2003.
[10] Ostachowicz WM, Krawczuk M. Analysis of the effect of cracks on the natural frequencies of a cantilever beam. J Sound Vibr 1991;150:191–201.
[11] Rosales MB, Filipich CP, Conca MA. Crack detection in a spinning beam. In: ENIEF 2004. Buscaglia G, Dari E, Zamonsky OI, editors. Mecanica computacional, vol. XXIII. 2004. p. 843–54.
[12] Rosales MB, Filipich CP, Buezas FS. Crack detection in beam-like structures using a power series technique and artificial neural networks. In: Proc. of the thirteenth international congress on sound and vibration. 2006.
[13] Filipich CP, Maurizi MJ, Rosales MB. Free vibrations of a spinning uniform beam with ends elastically restrained against rotation. J Sound Vibr 1987;116: 475–82.
[14] Bauer HF. Vibration of a rotating uniform beam, part I: Orientation in the axis of rotation. J Sound Vibr 1980;72:177–89.
[15] ALGOR Software. Version 4. Algor Inc., Pittsburgh, USA. 1997.
[16] Nelles O. Nonlinear systems identification. Heidelberg (Berlin): Springer; 2001.
[17] Buezas FS, Rosales MB, Filipich CP. Crack detection by means of static and dynamic simulations with a crack contact model. In: 8th. world congress on computational mechanics. 5th European congress on computational methods in applied sciences and engineering. 2008.